Intramolecular Electronic Energy Transfer in Ruthenium(II) Diimine Donor/Pyrene Acceptor Complexes Linked by a Single C−C Bond

Jerald A. Simon,[†] Steven L. Curry,[†] Russell H. Schmehl,*[,†] Timothy R. Schatz,[‡] Piotr Piotrowiak,[‡] Xiaoqing Jin,[§] and Randolph P. Thummel*[,§]

Contribution from the Departments of Chemistry, Tulane University, New Orleans, Louisiana 70118, Rutgers University, Newark, New Jersey 07102, and University of Houston, Houston, Texas 77204

Received January 8, 1997[⊗]

Abstract: The photophysical behavior of $[(bpy)_2Ru(L)]^{2+}$ complexes (L = 4-(1″-pyrenyl)-2,2′-bipyridine, **bpy-pyr**; 2-(1′-pyrenyl)-1,10-phenanthroline, **phen-pyr**; and 2-(2′-naphthyl)-1,10-phenanthroline, **phen-nap**) was investigated in solutions and frozen matrices. The conformation of the linked pyrene differs in the two complexes: The pyrene moiety is conformationally constrained to be nearly perpendicular to the phenanthroline in the **phen-pyr** complex while the pyrene in the **bpy-pyr** complex has much greater flexibility about the C−C bond linking the ligand and the pyrene. The ^{3}MLCT excited state of the Ru(II) diimine complex and the $^3(\pi \rightarrow \pi^*)$ state of the pyrenyl substituent are nearly isoenergetic; the ^{3}MLCT state is the lowest energy state in the **bpy-pyr** complex, and the pyrene $^3(\pi \rightarrow \pi^*)$ state is lower in energy for the **phen-pyr** complex. The **bpy-pyr** complex is unique in that the ^{3}MLCT state has a very long lived luminescence (approximately 50 μs in degassed CH_3CN). Luminescence decays for both pyrene containing complexes can be fit as double exponentials, indicating that the ^{3}MLCT and $^3(\pi \rightarrow \pi^*)$ states are not in equilibrium. Analysis of decays obtained at several temperatures reveal that energy transfer is slower than relaxation of the ^{3}MLCT state but more rapid than decay of the pyrene localized $^3(\pi \rightarrow \pi^*)$ state. The results also suggest that electronic coupling between the two states is weak despite the fact that the two chromophores are separated by a single covalent bond.

Introduction

Experimental studies of intramolecular triplet energy and electron transfer reactions have allowed detailed questions regarding the distance dependence, solvation, and free energy dependence of these reactions to be addressed. Much of the work has been used to provide quantitative tests of theoretical formalisms developed to describe this class of reactions. It has been clearly demonstrated that rate constants for electron transfer and triplet energy transfer reactions of organic donor−acceptor systems are a function of the degree of electronic interaction of the reactants. Rate constants generally decrease exponentially with increasing separation of the donor and acceptor moieties, and the magnitude of this decrease depends intimately on the nature of the covalent network bridging the donor and acceptor. An additional consideration, which has received less attention, is the effect of donor and acceptor conformation on electronic coupling, both with respect to the relative orientation of the donor and acceptor to one another and the orientation of both the donor and acceptor to the bridging component of the system. In examining photoinduced intramolecular charge separation and recombination reactions in covalently linked porphyrin/quinone systems, Wasielewski and co-workers associated differences in rate constants between spiro-pentane-bridged and trans-decalin-bridged complexes with differences in electronic coupling due to orientation.[1] McLendon's group and others, stimulated by results of Marcus, Cave, and Seiders on the nature of the torsion angle dependence of electronic coupling in phenyl-bridged bis-(porphyrin) complexes,[2] examined the effect of controlling the torsion angle between phenyl rings of a biphenyl-bridged bis-(porphyrin) donor−acceptor system.[3,4] Other studies of donor/acceptor orientation on electron transfer reactions have been published by Verhoeven and by Gust, Moore, and co-workers.[5,6] The limited number of studies in this area is due in part to the difficulty in preparing systems having well-defined geometries.

One potential approach for interrogating the influence of conformation on exchange energy transfer reactions is to employ transition metal complexes having bi- or tridentate coordinated ligands which can serve as either energy donors or acceptors. The coordination environment of the metal complex can be employed to lock the conformation of the associated ligand (donor/acceptor). The system can be used to examine intramolecular energy transfer as long as the metal complex and coordinated ligand have well-characterized excited states of known energy and the excited states are spatially isolated in a well-defined way. Several complexes are known which have luminescent metal-to-ligand charge transfer (MLCT) excited

[†] Tulane University.
[‡] Rutgers, Newark.
[§] University of Houston.
[⊗] Abstract published in *Advance ACS Abstracts,* October 15, 1997.

(1) (a) Sakata, Y.; Tsue, H.; O'Neil, M. P.; Wiederrecht, G. P.; Wasielewski, M. R. *J. Am. Chem. Soc.* **1994**, *116*, 6904. (b) Wasielewski, M.; Niemczyk, M. P.; Johnson, D. G.; Svec, W. A.; Minsek, D. W. *Tetrahedron* **1989**, *45*, 4785. (c) Wasielewski, M. R.; Johnson, D. G.; Niemczyk, M. P.; Gaines, G. L.; O'Neil, M. P.; Svec, W. A. *J. Am. Chem. Soc.* **1990**, *112*, 6482.

(2) (a) Cave, R. J.; Siders, P.; Marcus, R. A. *J. Phys. Chem.* **1986**, *90*, 1436. (b) Siders, P.; Cave, R. J.; Marcus, R. A. *J. Chem. Phys.* **1984**, *81*, 5613.

(3) Helms, A.; Heiler, D.; McLendon, G. L. *J. Am. Chem. Soc.* **1991**, *113*, 4325.

(4) Osuka, A.; Maruyama, K.; Mataga, N.; Asahi, T.; Yamazaki, I.; Tamai, N. *J. Am. Chem. Soc.* **1990**, *112*, 4958.

(5) (a) Overing, H.; Verhoeven, J. W.; Paddon-Row, M. N.; Warman, J. M. *Tetrahedron* **1989**, *45*, 4751. (b) Oliver, A. M.; Craig, D. C.; Paddon-Row, M. N.; Kroon, J.; Verhoeven, J. W. *Chem. Phys. Lett.* **1988**, *150*, 366.

(6) Gust, D.; Moore, T. A.; Moore, A. L.; Devadoss, C.; Liddell, P. A.; Hermant, R.; Nieman, R. A.; Demanche, L. J.; DeGraziano, J. M.; Gouni, I. *J. Am. Chem. Soc.* **1992**, *114*, 3590.

S0002-7863(97)00069-3 CCC: $14.00

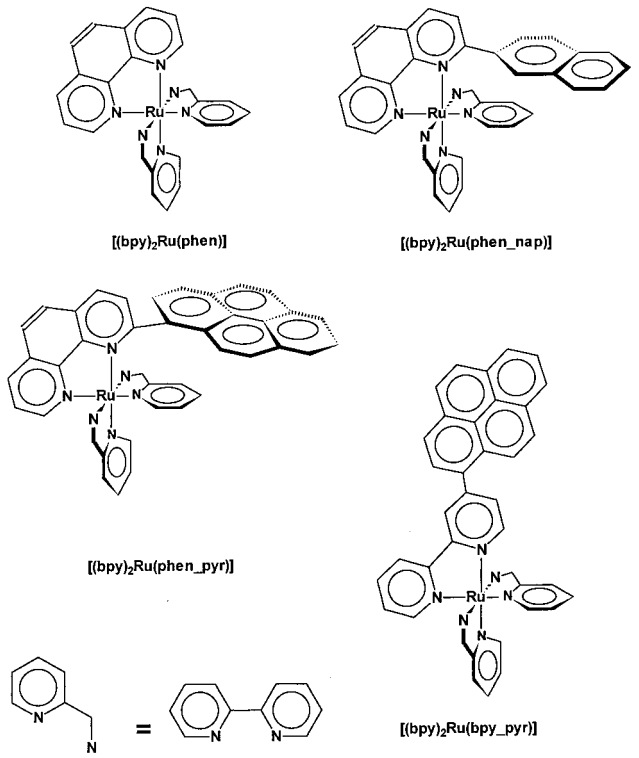

Figure 1. Structures of the ligands and complexes studied.

states and coordinated ligands in fixed orientations which exhibit ligand localized (IL) phosphorescence in low-temperature matrices.[7−9] In most of these systems the IL excited state is in intimate contact with the metal center (i.e. $[(CO)_3(CH_3CN)Re(bpy\text{-}sty)]^+$; bpy-sty = 1-phenyl-2-(2,2′-bipyrid-4-yl)ethene). The MLCT transition in complexes of this type is often localized on the ligand having an IL excited state with an energy less than or equal to that of the MLCT state. Very recently we have prepared the ligands **phen-nap**, **phen-pyr**, and **bpy-pyr** (Figure 1) and the corresponding complexes $[(bpy)_2Ru(L)](PF_6)_2$ (bpy = 2,2′-bipyridine). The naphthyl and pyrenyl moieties linked to the phenanthroline ligand are oriented nearly perpendicular to the phenanthroline ligand in the Ru(II) complexes as a result of steric restraint imposed by the spectator bipyridine ligands. The **bpy-pyr** complex is able to adopt conformations bringing it closer to planarity with the bipyridine ligand. Recent work of Ford and Rodgers[10] as well as Wilson, Sasse, and Mau[11] illustrated definitively that reversible exchange energy transfer occurs between Ru(II) → diimine ^{3}MLCT states and triplet pyrene covalently linked to the complex via an alkyl tether. In this work a detailed discussion of the photophysical behavior of the Ru(II) complexes of **bpy-pyr**, **phen-pyr**, and **phen-nap** is presented. Examination of temperature-dependent luminescence decays of the linked pyrene complexes allows evaluation of rate constants for exchange energy transfer from the ^{3}MLCT excited state of the complex to the $^3(\pi \rightarrow \pi^*)$ state of the linked pyrene. Activation parameters obtained for both the **bpy-pyr** and **phen-pyr** complexes indicate the ^{3}MLCT and $^3(\pi \rightarrow \pi^*)$ states are weakly coupled. The implication is that conformational restraint in the **phen-pyr** complex is not the major factor influencing the very weak electronic coupling in these systems.

Experimental Section

Syntheses. The ligands **phen-nap** and **phen-pyr** and the complex $[(bpy)_2RuCl_2]$ were prepared according to previously published methods.[17] Solvents used were reagent grade.

4-(1-Pyrenyl)-2,2′-bipyridine (bpy-pyr). To a solution of 1-pyrenecarbaldehyde (4.01 g, 0.0174 mol) in absolute ethanol (1.1 L), deionized water (0.3 L) was slowly added, and the ethanol/water solution was allowed to cool to room temperature. A solution of pyruvic acid sodium salt (5.63 g, 0.0512 mol) in water (50 mL) was slowly added, and the solution was immersed in an ice bath and maintained at 5−10 °C. To the slightly cloudy solution, KOH (10.97 g, 0.195 mol) in water (25 mL) was added dropwise, and the solution turned bright orange. The cloudy slurry was allowed to stir for 0.5 h, and additional KOH (9.67 g, 0.17 mol) in water (25 mL) was added. The mixture was allowed to stir for an additional 2 h, acidified to pH 6 with 20% aqueous HCl, and then removed from the ice bath and stirred at room temperature for 1 h. The precipitate was filtered out and washed with cold water followed by cold ethanol. Drying in a vacuum oven at 85 °C overnight gave 1-(3-carboxyl-3-oxoprop-1-enyl)-pyrene as a dark orange solid (4.05 g, 77%) which was used directly without further purification.

The crude 1-(3-carboxyl-3-oxoprop-1-enyl)pyrene (4.00 g, 0.0133 mol), 2-acetylpyridine pyridinium hexafluorophosphate (5.2 g, 0.0152 mol), and ammonium acetate (7.9 g, 0.102 mol) were added to water (150 mL) and refluxed for 9 h under Ar. The precipitate was filtered out and washed several times with water and acetone. The light orange solid was dried overnight in a vacuum oven at 60 °C to yield 2.76 g of crude 4-(1-pyrenyl)-6-carboxy-2,2′-bipyridine. A portion of this solid (1 g, 0.0025 mol) was added to a 50 mL RB flask with an equal volume of fine sand and mixed thoroughly. The flask was placed in a preheated sand bath at a temperature of 190 °C and heated under vacuum for 30 min. The product was collected from the bottom of the flask by dissolving in $CHCl_3$; any undissolved material was removed by filtration, and decolorizing charcoal was added to the dark brown solution, which was heated for 10 min and filtered. The light brown solution was flash chromatographed on Al_2O_3 using $CHCl_3$ as eluent. A dark band remained at the top of the column and the first light yellow band was collected. The solvent was evaporated to yield **bpy-pyr** as a light brown solid (0.704 g, 15%): ^{1}H NMR ($CDCl_3$) δ 7.33 (dq, 1H, J = 1.37, 4.79, 13.9 Hz), 7.59 (dd, 1H, J = 1.7, 5.13 Hz), 7.87 (dt, 1H, J = 1.7, 7.8, 13.9 Hz), 8.01−8.25 (multiplet, 9H), 8.52 (d, 1H, J = 7.8 Hz), 8.68 (dd, 1H, J = 1.7, 4.8 Hz), 8.72 (d, 1H, J = 1.7 Hz), 8.86 (d, 1H, J = 5.1 Hz).

$[(bpy)_2Ru(bpy\text{-}pyr)](PF_6)_2$. A mixture of **bpy-pyr** (71 mg, 0.2 mmol) and $[(bpy)_2RuCl_2]$ (48 mg, 0.10 mmol)[12] was dissolved in 2-butanol (25 mL) and refluxed under N_2 for 5 h. During the reaction the color changed from dark purple to a dark yellow/brown. The solvent was evaporated *in vacuo* and the residue dissolved in water. The unreacted ligand was removed by filtration, and aqueous NH_4PF_6 was added to the filtrate to precipitate the complex. This material was dried and then chromatographed on Al_2O_3 eluting first with CH_3CN/toluene (1:4 followed by 1:1). The latter eluent produced a dark orange band which contained the desired complex (70 mg, 33%). ^{1}H NMR (CD_3CN): δ 8.80 (d, 1H), 8.6−8.5 (m, 5 H), 8.4−8.3 (m, 4 H), 8.23 (m, 4 H), 8.15−8.0 (m, 8 H), 7.9−7.75 (m, 6 H), 7.68 (dd, 1 H), 7.57 (t, 1 H), 7.52−7.4 (m, 5 H), 7.24 (t, 1 H), 7.18−7.13 (m, 1 H). Anal. Calcd for $C_{46}H_{32}N_6RuP_2F_{12}$·toluene: C, 55.26; H, 3.50; N, 7.29. Found: C, 54.46; H, 3.56; N, 7.04.

$[(bpy)_2Ru(phen\text{-}pyr)](PF_6)_2$. A mixture of **phen-pyr** (64.7 mg, 0.17 mmol) and $[(bpy)_2RuCl_2]$ (80.7 mg, 0.15 mmol) in absolute ethanol (7 mL) was refluxed under Ar for 16 h. After cooling, excess NH_4PF_6 was added, and the resulting precipitate was collected and purified by chromatography on Al_2O_3 using CH_3CN/ toluene (1:1) to provide an orange-red solid (120 mg, 74%). HPLC showed a major peak with a retention time of 3.95 min and no contamination by $[Ru(bpy)_3](PF_6)_2$.

(7) (a) Fredericks, S. M.; Luong, J. C.; Wrighton, M. S. *J. Am. Chem. Soc.* **1979**, *101*, 7415. (b) Wrighton, M. S.; Morse, D. L.; Pdungsap, L. *J. Am. Chem. Soc.* **1975**, *97*, 2073.

(8) (a) Taffarel, E.; Chirayil, S.; Kim, W. Y.; Thummel, R. P.; Schmehl, R. H. *Inorg. Chem.* **1996**, *35*, 2127. (b) Baba, A. I.; Ensley, H. E.; Schmehl, R. H. *Inorg. Chem.* **1995**, *34*, 1198. (c) Shaw, J. R.; Schmehl, R. H. *J. Am. Chem. Soc.* **1991**, *113*, 389. (d) Shaw, J. R.; Webb, R. T.; Schmehl, R. H. *J. Am. Chem. Soc.* **1990**, *112*, 1117.

(9) (a) Sacksteder, L.; Lee, M.; Demas, J. N.; DeGraff, B. A. *J. Am.Chem. Soc.* **1993**, *115*, 8230. (b) Wang, Z.; Lees, A. J. *Inorg. Chem.* **1993**, *32*, 1493.

(10) Ford, W. E.; Rodgers, M. A. J. *J. Phys. Chem.* **1992**, *96*, 2917.

(11) Wilson, G. J.; Sasse, W. H. F.; Mau, A. W.-H. *Chem. Phys. Lett.* **1996**, *250*, 583.

(12) Sullivan, B. P.; Salmon, D. J.; Meyer, T. J. *Inorg. Chem.* **1978**, *17*, 3334.

^{1}H NMR (CD_3CN) showed major and minor peaks in an approximate 3:1 ratio indicating the existence of two diasteromers: δ 8.85 (d, 1H), 8.66 (d, 1H), 8.61 (d), 8.45−7.0 (overlapping m), 6.56 (d, 1 H), 6.35 (q), 6.30 (d), 6.14 (m). Anal. Calcd for $C_{48}H_{32}N_6RuP_2F_{12}$: C, 53.19; H, 2.96; N, 7.76. Found: C, 53.17; H, 2.88; N, 7.62.

[(bpy)$_2$Ru(phen-nap)](PF$_6$)$_2$. A mixture of **phen-nap** (100 mg, 0.326 mmol) and [(bpy)$_2$RuCl$_2$] (204 mg, 0.392 mmol) in absolute ethanol (40 mL) was refluxed under Ar for 16 h. After cooling, excess NH_4PF_6 was added and the resulting precipitate was collected and purified by chromatography on Al_2O_3 using CH_3CN/ toluene (1:1) to provide an orange-red solid (228 mg, 70%). Recrystallization from CH_3CN/ toluene gave [(bpy)$_2$Ru(**phen-nap**)](PF$_6$)$_2$ as red crystals. HPLC showed a major peak with a retention time of 3.76 min and no contamination by [Ru(bpy)$_3$](PF$_6$)$_2$. ^{1}H NMR (CD_3CN) showed major and minor peaks in approximate 85:15 ratio indicating the existence of two diastereomers: δ 8.75 (d, 1H), 8.63 (d, 1H), 8.34 (overlapping m), 8.13 (t, 1 H), 7.99 (t, 1 H), 7.95−7.2 (overlapping m), 6.95 (d, overlapping t), 6.80 (dd, 1 H), 6.48 (s), 6.41 (t), 6.20 (d), 6.01 (t). Anal. Calcd for $C_{42}H_{30}N_6RuP_2F_{12}$: C, 49.91; H, 2.97; N, 8.32. Found: C, 50.06; H, 2.92; N, 8.39.

Physical Measurements. Nuclear magnetic resonance spectra were recorded for **bpy-pyr** on a GE QE-400 spectrometer and for [(bpy)$_2$Ru(**phen-pyr**)](PF$_6$)$_2$ and [(bpy)$_2$Ru(**phen-nap**)](PF$_6$)$_2$ on a GE QE-300. Chemical shifts are reported in parts per million downfield from TMS. Cyclic voltammograms were recorded using either a BAS CV-27 or an EG&G Versastat according to procedures described earlier.[13] Potentials were determined relative to SSCE reference. HPLC was performed using a Waters Protein-Pak SP 5PW steel column (7.5 × 75 mm), eluting with CH_3CN/ 0.03 M aqueous KH_2PO_4 (7:3) at 1.5 mL/min.

Absorption spectra were obtained using a HP8452 diode array spectrophotometer. Steady-state luminescence spectra were obtained using a SPEX fluorolog equipped with a 450 W Xe arc lamp, thermostated cell holder, and cooled PMT housing. Room-temperature luminescence decays of the **phen-nap** and **phen-pyr** complexes were obtained by time correlated single-photon counting using an apparatus described earlier.[8a] Time-resolved emission spectra were collected using a spectrograph/gated, image intensified diode array detector triggered by excitation pulses from a N_2 laser (Laser Photonics, LN 1000). The image-intensified diode array had an instrumental delay of 100 ns and a minimum gate window of 100 ns. Luminescence lifetimes between 77 K and room temperature were acquired using N_2 pumped dye laser excitation (using Coumarin 460 at 460 nm), filtering the emitted light through a Heath-McPherson Model EU-700 monochromator and detecting the emitted light with a Hammamatsu R 928 PMT. Decays typically represented the average of 100−500 pulses and were collected on a Hewlett Packard Model 54111D digital oscilloscope. Luminescence decays were analyzed either as simple single or double-exponential decays using a modified Marquardt algorithm written in-house or using an excited-state equilibrium model as described below. Transient absorption spectra were obtained using doubled output from a Nd:YAG laser for excitation with a pulsed flashlamp−monochromator−germanium photodiode detector for observing transient absorbance changes. The apparatus has been described in detail elsewhere.[14]

Luminescence decays of [(bpy)$_2$Ru(**phen-pyr**)](PF$_6$)$_2$ and [(bpy)$_2$Ru(**bpy-pyr**)](PF$_6$)$_2$ at temperatures between 100 and 200 K were fit to a model involving relaxation from both the ^{3}MLCT and ^{3}**pyr** excited states (eq 1). The decay pathways following excitation into the ^{1}MLCT

$$[(bpy)_2Ru^{III}(\mathbf{phen^-\text{-}pyr})](PF_6)_2 \rightleftharpoons [(bpy)_2Ru^{II}(\mathbf{phen\text{-}*pyr})](PF_6)_2 \quad (1)$$
$$^3\text{MLCT} \qquad\qquad ^3\text{IL}$$

state are shown in Scheme 1; included are the possibility of ^{3}MLCT to ^{3}MC internal conversion and intersystem crossing from the ^{1}MLCT state to both the ^{3}MLCT and ^{3}**pyr** states. Luminescence data files were normalized and then fit using a Simplex algorithm.[15] The routine uses

Scheme 1

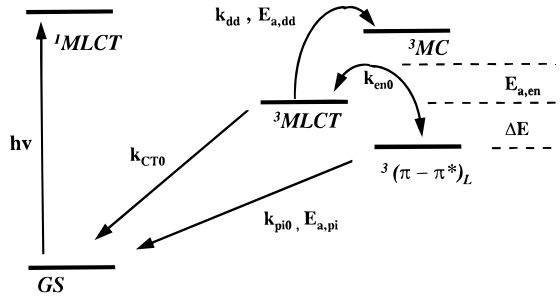

a fourth-order Runge−Kutta algorithm[16] to numerically integrate the differential kinetic equations for the appropriate kinetic models shown in Scheme I. The software was written in FORTRAN, and the programs were run on an IBM RISC-6000 computer.

Relative quantum yields for photosubstitution were obtained for the complexes in methylene chloride solutions containing tetraethylammonium chloride (1 mM). Samples were N_2 bubble degassed prior to photolysis at 450 nm using filtered output from a 450 W Xe arc lamp. Quantum yields were calculated by observing the growth of the absorbance of the cis-chloro product which has an absorption maximum at 550 nm.

Results

Syntheses. [Ru(bpy)$_2$Cl$_2$] was prepared according to a published procedure as were the ligands 2-(2′-naphthyl)-1,10-phenanthroline (**phen-nap**) and 2-(1′-pyrenyl)-1,10-phenanthroline (**phen-pyr**).[17] The ligand **bpy-pyr** was made by the initial Michael addition of pyruvic acid to pyrene-1-carbaldehyde followed by the Hantzsch−Kröhnke reaction reaction with 2-acetylpyridine pyridinium hexafluorophosphate in the presence of ammonium acetate to yield the bipyridine-6-carboxylic acid.[18] This material was decarboxylated via pyrolysis in a sublimator to yield **bpy-pyr**. Complexes of the type [(bpy)$_2$Ru(L)](PF$_6$)$_2$ were prepared by reaction of the ligands with [Ru(bpy)$_2$Cl$_2$] in water/ethanol mixtures. The complexes were purified by column chromatography on alumina to remove unreacted ligand, remaining cis-chloro complex, and traces of [Ru(bpy)$_3$](PF$_6$)$_2$.

Electrochemistry. The redox behavior of the complexes was examined by cyclic voltammetry and differential pulse polarography in acetonitrile solutions. The parent complex [(bpy)$_2$Ru(phen)]$^{2+}$ exhibits a single chemically and electrochemically reversible oxidation with an $E^{\circ\prime}$ of 1.23 V vs SCE and three reversible reductions at potentials more positive than −2.0 V vs SCE.[19] Detailed electrochemical studies of Ru(II) tris(diimine) complexes have clearly shown that the one electron oxidation of the complex is metal centered[20] (oxidation to Ru(III)). The three reductions result from successive reduction of each coordinated diimine ligand; this has been demonstrated via ESR, and spectroelectrochemical methods.[21,22] The complexes having **phen-pyr** and **bpy-pyr** ligands exhibit quasi-reversible voltammograms for both oxidative and reductive redox reactions. Figure 2 shows a typical cyclic voltammogram for **bpy-pyr** and [(bpy)$_2$Ru(**bpy-pyr**)]$^{2+}$ in acetonitrile at room

(13) (a) Goulle, V.; Thummel, R. P. *Inorg. Chem.* **1990**, *29*, 1767. (b) Liang, Y. Y.; Baba, A. I.; Kim, W. Y.; Atherton, S. J.; Schmehl, R. H. *J. Phys. Chem.* **1996**, *100*, 18408.

(14) Strati, G.; Piotrowiak, P. *J. Photochem. Photobiol. A: Chem.*, in press.

(15) Demas, J. *Excited State Lifetime Measurements*; Academic Press: New York, 1983; Chapter 4.

(16) Shoup, T. *A Practical Guide to Computer Methods for Engineers*; Prentice-Hall: Englewood Cliffs, NJ, 1979; p 73.

(17) Riesgo, E. C.; Jin, X.; Thummel, R. P. *J. Org. Chem.* **1996**, *61*, 3017.

(18) (a) Krohnke, F. *Synthesis* **1976**, 1. (b) Baba, A. I.; Wang, W.; Kim, W. Y.; Strong, L. A.; Schmehl, R. H. *Synth. Commun.* **1994**, *24*, 1029.

(19) Caspar, J. V.; Meyer, T. J. *Inorg. Chem.* **1983**, *22*, 2444.

(20) (a) Juris, A.; Balzani, V.; Barigelletti, F.; Campagna, S.; Belser, P.; von Zelewsky, A. *Coord. Chem. Rev.* **1988**, *82*, 85. (b) Tokel-Trkvoryan; Hemingway, R. E.; Bard, A. J. *J. Am. Chem. Soc.* **1973**, *95*, 6582.

(21) Morris, D.; Hanck, K.; DeArmond, M. *J. Am. Chem. Soc.* **1983**, *105*, 3032.

(22) (a) Elliott, C..; Hershenhart, E. *J. Am. Chem. Soc.* **1982**, *104*, 7519. (b) Heath, G.; Yellowlees, L.; Braterman, P. *J. Chem. Soc., Chem. Commun.* **1981**, 287.

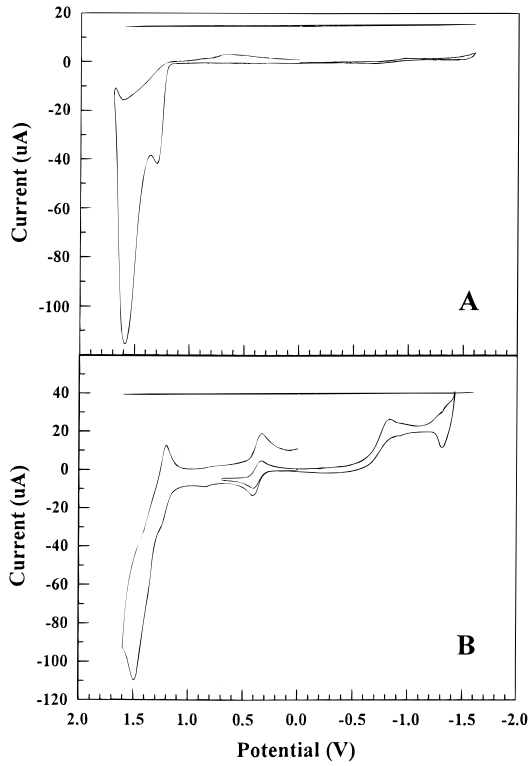

Figure 2. Cyclic voltammograms of (A) **phen-pyr** and (B) [(bpy)$_2$Ru(**phen-pyr**)]$^{2+}$ in CH_3CN at room temperature with tetraethylammonium perchlorate electrolyte and ferrocene internal reference (shown in B).

temperature. The ligand exhibits irreversible oxidation at voltages more positive than 1.1 V vs SCE; irreversible oxidation of pyrene derivatives in the presence of even weak nucleophiles is well documented, and the chemistry following oxidation involves reaction at the 1, 3, 6 and 8 positions.[23] Pyrene oxidation in liquid SO_2 is reversible and has an $E°$ of 1.26 V vs SCE at −52 °C.[24] The Ru(II) complexes of **bpy-pyr** and **phen-pyr** have quasi-reversible oxidations ($E° \sim 1.3$ V vs SCE) in which the anodic current is much greater than the cathodic current. This behavior reflects the fact that the Ru(II) and coordinated **bpy-pyr** are oxidized at very similar potentials and the Ru(III) is stable while the oxidized **bpy-pyr** undergoes irreversible chemistry. No attempt was made to perform controlled potential electrolysis and product analysis to identify the oxidation products.

No reductive waves were observed in cyclic voltammograms of **bpy-pyr** or **phen-pyr** at potentials more positive than −1.7 V. Reversible reduction of pyrene occurs with an $E°$ of −2.17 V vs SCE in dimethylamine at −40 °C.[25] The first reduction in cyclic voltammograms of [(bpy)$_2$Ru(**bpy-pyr**)]$^{2+}$ has a cathodic current peak at −0.8 V which is irreversible. Reduction of the **phen-pyr** complex also exhibits irreversible reduction at potentials more positive than −1.0 V. The complex [(bpy)$_2$Ru(**phen-nap**)]$^{2+}$ has two reversible reductions between 0 and −1.7 V; these observations suggest that reduction of the **phen-pyr** and **bpy-pyr** complexes is irreversible due to chemistry at the pyrene.

Electronic Spectra. The absorption spectra of **bpy-pyr** and **phen-pyr** are structureless and therefore differ from the spectra of pyrene and 1-alkylpyrenes which exhibit distinct vibrational structure.[26] Absorption spectral data for the ligands and complexes in acetonitrile are given in Table 1. By comparison

Table 1. Electronic Absorption Spectral Maxima (CH_3CN, 25 °C)

compd	λ_{max}, nm	ϵ (M^{-1} cm^{-1})	transition
phen-nap	315	36 300	($\pi \rightarrow \pi^*$)
	277	61 600	($\pi \rightarrow \pi^*$)
phen-pyr	360	16 500	($\pi \rightarrow \pi^*$) pyrene
	280	25 500	($\pi \rightarrow \pi^*$)
bpy-pyr	342	25 510	($\pi \rightarrow \pi^*$) pyrene
	280	45 700	($\pi \rightarrow \pi^*$)
[(bpy)$_2$Ru(**phen-nap**)]$^{2+}$	448	16 600	MLCT [Ru(dπ) → L(π^*)]
	288	57 500	($\pi \rightarrow \pi^*$)
[(bpy)$_2$Ru(**phen-pyr**)]$^{2+}$	451	12 600	MLCT [Ru(dπ) → L(π^*)]
	334	15 500	($\pi \rightarrow \pi^*$) pyrene
	286	41 700	($\pi \rightarrow \pi^*$)
[(bpy)$_2$Ru(**bpy-pyr**)]$^{2+}$	456	20 200	MLCT [Ru(dπ) → L(π^*)]
	340	31 200	($\pi \rightarrow \pi^*$) pyrene
	288	88 450	($\pi \rightarrow \pi^*$)

with the vast number of Ru(II) diimine complexes reported, the lowest energy electronic transition in all the metal complexes is Ru(dπ) → diimine(π^*) MLCT,[20] although it is not clear whether the transition is to the derivatized phen/bpy ligand or Ru(dπ) → bpy(π^*). The fact that the MLCT transition of [(bpy)$_2$Ru(**bpy-pyr**)]$^{2+}$ is at lower energy than the parent complex, [(bpy)$_3$Ru]$^{2+}$ (Table 2), suggests the MLCT transition is to the **bpy-pyr** ligand.

Room-Temperature Photophysical Behavior. Emission maxima, lifetimes, quantum yields, and radiative decay rate constants for the complexes are listed in Table 2. The parent complexes, [(bpy)$_2$Ru(phen)]$^{2+}$ and [Ru(bpy)$_3$]$^{2+}$, exhibit red luminescence with an efficiency of approximately 10% in acetonitrile, and lifetimes for solutions of these complexes are on the order of 600 ns to 1 μs.[20] Excited-state absorption spectra of both the parent complexes are characterized by a strong absorption with a maximum of approximately 360 nm and bleaching of the ground state in the 400−500 nm wavelength region, and an additional, very weak absorbance is observed above 500 nm.

The complexes having substituents in the 2-position of the coordinated phenanthroline, [(bpy)$_2$Ru(**phen-nap**)]$^{2+}$ and [(bpy)$_2$Ru(**phen-pyr**)]$^{2+}$, both exhibit much weaker luminescence and have much shorter luminescence lifetimes than the parent complex; the calculated radiative decay rate constants (Table 2) are on the order of 10^5 s^{-1} consistent with emission from a ^{3}MLCT state. The transient absorption spectrum of [(bpy)$_2$Ru(**phen-nap**)]$^{2+}$ was difficult to obtain using our apparatus because of the very short excited-state lifetime, but bleaching in the 400−500 nm region is observed. For [(bpy)$_2$Ru(**phen-pyr**)]$^{2+}$ a transient having the spectrum shown in Figure 3a was observed; the lifetime of the transient was approximately 15 times longer than the luminescence lifetime. The spectrum is completely different from that of the parent complex but closely resembles the spectrum of a complex which contains pyrene covalently linked to [Ru(bpy)$_2$(phen)]$^{2+}$ by an aliphatic tether.[10] One concern is that the weak luminescence observed emanates from an impurity. Several factors suggest the weak luminescence is from the **phen-pyr** complex rather than an impurity. First, the calculated radiative decay rate constant (ϕ_{em}/τ_{em}) is very similar to that of a large number of Ru(II) diimine complexes. The most likely impurity is [Ru(bpy)$_3$]$^{2+}$; however, the luminescence lifetime would be approximately 800 ns if [Ru(bpy)$_3$]$^{2+}$ was the emitting species. Other plausible impurities, such as [Ru(bpy)$_2$Cl$_2$] and [Ru(bpy)$_2$(CH$_3$CN)$_2$]$^{2+}$, are nonemissive in room-temperature acetonitrile. Finally, the complex has been shown to be pure by HPLC, under conditions where [Ru(bpy)$_3$]$^{2+}$ and other similar impurities are easily distinguished.

(23) See for example: (a) Adams, R. N. *Electrochemistry at Solid Electrodes*; Dekker: New York, 1969; pp 308−14. (b) Weinberg, N. L.; Weinberg, H. R. *Chem. Rev.* **1968**, *68*, 449.

(24) Dietrich, M.; Heinze, J. *J. Am. Chem. Soc.* **1990**, *112*, 5142.

(25) Meerholz, K.; Heinze, J. *J. Am. Chem. Soc.* **1989**, *111*, 2325.

(26) See: Murov, S.; Carmichael, I.; Hug, G. *Handbook of Photochemistry*; Dekker: New York, 1993; p 184.

Table 2. Absorption and Luminescence Characteristics of Complexes[a]

complex	λ_{max}, nm MLCT	$E_{em}(298)$, nm	$\phi_{em}(298)$	$\tau_{em}(298)$ ns	$\tau_{TA}(298)$,[b] ns	$\eta_{isc}k_r$, 10^{-4} s^{-1}	$E_{em}(77)$, nm	$\tau_{em}(77)$, μs
$[(bpy)_2Ru(\mathbf{phen})]^{2+}$	448	600	0.069	700	700	9.5	585	5
$[(bpy)_2Ru(\mathbf{phen\text{-}nap})]^{2+}$	448	611	0.0005	3[5]	5	14	583	4.8
$[(bpy)_2Ru(\mathbf{phen\text{-}pyr})]^{2+}$	450	610	0.0009	4	68	22	601	5.3
								5200
$[Ru(bpy)_3]^{2+}$ [c]	451	620	0.086	860		10	580	5.0
$[(bpy)_2Ru(\mathbf{bpy\text{-}pyr})]^{2+}$	456	640	0.10	1 300		7.5	627	4.1
				57 400		(0.17)[d]		650

[a] Quantum yields ±15%; lifetimes less than 10 ns ± 50%; lifetimes > 10 ns ± 5%; TA lifetimes ± 10%; emission maxima ± 2 nm. 77 K data obtained in 4:1 ethanol/methanol glasses. Room-temperature data in CH_3CN. [b] Lifetime obtained from excited-state absorption. λ_{ex} = 532 nm; λ_{obs} = 440 nm. [c] Kawanishi, Y.; Kitamura, N.; Kim, T.; Tazuke, S. *Riken. Q.* **1984**, *78*, 212 and ref 14a. [d] Value obtained using long lifetime component and luminescence quantum yield.

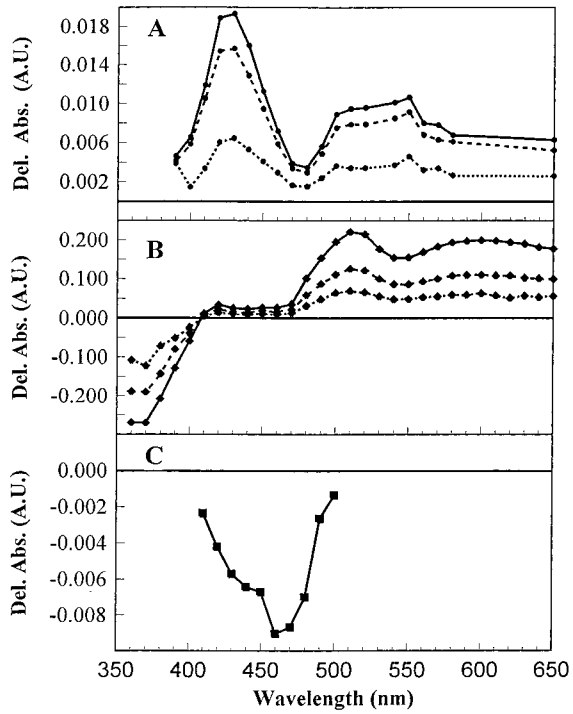

Figure 3. Excited-state absorption spectra of (A) $[(bpy)_2Ru(\mathbf{phen\text{-}pyr})]^{2+}$ at delays of 20 ns (—), 90 ns (- - -), and 200 ns (···), (B) $[(bpy)_2Ru(\mathbf{bpy\text{-}pyr})]^{2+}$ at delays of 70 ns (—), 270 ns (- - -), and 465 ns (···), and (C) $[(bpy)_2Ru(\mathbf{phen\text{-}nap})]^{2+}$ at a delay of 20 ns. Spectra were obtained in FPT degassed CH_3CN solutions at room temperature.

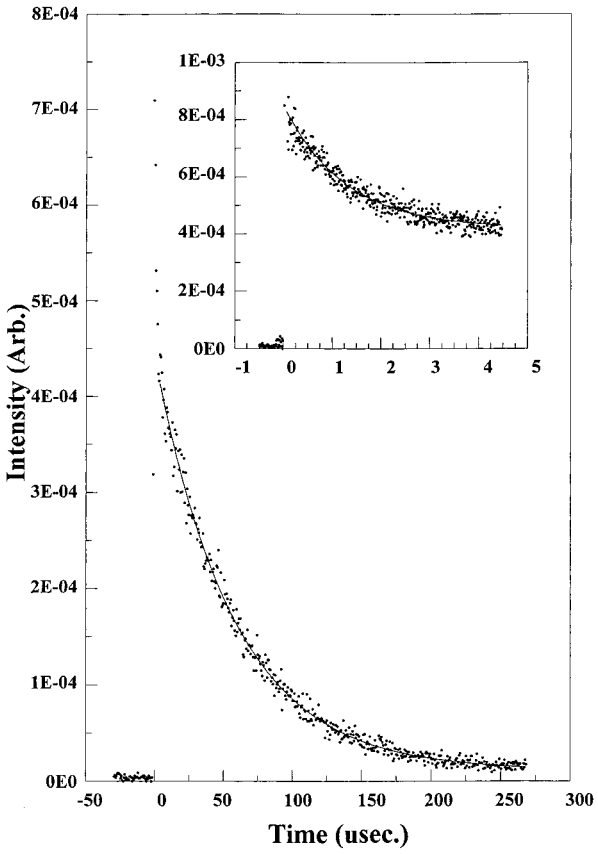

Figure 4. Room-temperature luminescence decay of $[(bpy)_2Ru(\mathbf{bpy\text{-}pyr})]^{2+}$ in FPT degassed CH3CN solution following dye laser excitation at 460 nm. Inset shows initial portion of the decay.

The complex having pyrene substituted in the 4 position of 2,2′-bipyridine, $[(bpy)_2Ru(\mathbf{bpy\text{-}pyr})]^{2+}$, exhibits luminescence of comparable efficiency but 20 nm to the red of the parent complex, $[Ru(bpy)_3]^{2+}$. The luminescence decay of the complex in freeze−pump−thaw degassed acetonitrile is double exponential (Figure 4); the predominant component has a lifetime of 57 μs, far longer than typical lifetimes for ^{3}MLCT states of Ru(II) diimine complexes.[20] Upon purging of solutions of the complex with air, the decay becomes a single exponential with a lifetime of 300 ns. The decay of transient absorption is also double exponential at all wavelengths, and the spectrum in acetonitrile (Figure 3) differs from that of the parent complex, $[Ru(bpy)_3]^{2+}$, and $[(bpy)_2Ru(\mathbf{phen\text{-}pyr})]^{2+}$. The spectrum obtained immediately following excitation exhibits bleaching between 350 and 400 nm (with a minimum at 370 nm), virtually no absorbance change between 410 and 470 nm, and two absorption bands farther to the red with maxima at 520 and 580 nm and nearly equal ΔA values. The spectrum evolves to one in which a net absorption is observed between 350 and 375 nm and the maximum of the band farthest to the red shifts to 610.

Luminescence between 77 K and Room Temperature. Both of the pyrene-containing ligands exhibit strong green fluorescence in room-temperature solutions and frozen matrices. No discussion of the fluorescence of these ligands will be presented here. Phosphorescence from the ligands can also be observed at 77 K in 4:1 ethanol/methanol glasses containing approximately 10% ethyl iodide. Figure 5 shows spectra of both ligands obtained at 77 K, and Table 3 provides values for E_{00} and the averaged vibrational progression obtained from the spectra.

Vast differences are observed in the 77 K emission spectra of $[(bpy)_2Ru(\mathbf{phen\text{-}nap})]^{2+}$, $[(bpy)_2Ru(\mathbf{phen\text{-}pyr})]^{2+}$, and $[(bpy)_2Ru(\mathbf{bpy\text{-}pyr})]^{2+}$, all shown in Figure 6. The **phen-nap** complex exhibits structured luminescence very similar to the ^{3}MLCT emission of $[(bpy)_2Ru(phen)]^{2+}$; the individual points represent the data and the solid line presents the spectrum obtained from a fit using a two-mode Franck−Condon analysis (*vide infra*); the spectral fitting parameters are given in Table 3. The luminescence decay of the **phen-nap** complex is single exponential at all temperatures examined between 77 K and room temperature; the lifetime at 77 K is 4.8 μs. The temperature dependence of the luminescence lifetime in CH_3CN solution was examined at temperatures above the freezing

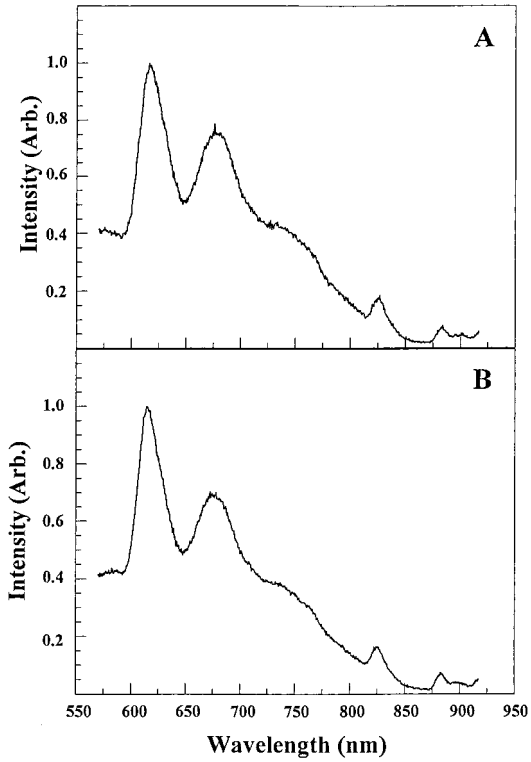

Figure 5. Phosphorescence spectra of (A) **bpy-pyr** and (B) **phen-pyr** in 4:1 ethanol/methanol with added ethyl iodide at 77 K.

Table 3. Spectral Fitting Parameters Obtained from Fits of 77 K Luminescence in 4:1 Ethanol/Methanol Glasses[a]

complex	E_0, cm^{-1}	$h\nu_M$, cm^{-1}	S_M	$\nu_{1/2}$, cm^{-1}
phen-pyr	~16 100	1460		~500
bpy-pyr	~16 300	1430		~500
[(bpy)$_2$Ru(**phen**)]$^{2+}$	17 200	1330	0.75	700
[(bpy)$_2$Ru(**phen-nap**)]$^{2+}$	17 300	1370	0.46	700
[(bpy)$_2$Ru(**phen-pyr**)]$^{2+}$	16 600	1350	0.05	380
[(bpy)$_2$Ru(**bpy-pyr**)]$^{2+}$	16 090	1390	0.48	800

[a] $h\nu_l = 450$ cm^{-1}; $S_l = 0.7 \pm 0.05$; values of $E_0 \pm 50$ cm^{-1}; $h\nu_M \pm 5\%$; $S_M \pm 10\%$; $\nu_{1/2} \pm 10\%$.

point of the solvent (Figure 7). The data were fit by assuming a single thermally activated nonradiative decay process (*vide infra*).

The emission spectrum of [(bpy)$_2$Ru(**phen-pyr**)]$^{2+}$ at 77 K is shown in Figure 6B. The narrow bandwidth of the principal emission component observed in the spectrum resembles the structured phosphorescence observed for unsubstituted pyrene and alkyl-substituted pyrenes but clearly differs from the relatively broad bands in the vibronic progressions observed in the emission spectra of the **phen-pyr** ligand (Figure 5) and the MLCT emission of [(bpy)$_2$Ru(phen)]$^{2+}$.[27] The luminescence decay of the complex in 4:1 ethanol/methanol at 77 K can be fit as a double exponential with components of 5.3 μs and 5.2 ms. Time-resolved emission spectra obtained less than 3 μs following excitation have the narrow band component and a broader emission characteristic of MLCT emission (Figure 8) while spectra taken with delays greater than 5 μs are superimposable with the steady-state spectrum. At temperatures above the solvent glass transition (approximately 120 K) the spectrum of the complex broadens and loses vibrational structure. The luminescence decays remain nonexponential above 77 K; three representative decays are shown in Figure 9. Above approximately 220 K luminescence decays for this complex can be fit as single exponentials; the temperature dependence of

(27) Ramamurthy, V.; Caspar, J. V.; Eaton, D. F.; Kuo, E. W.; Corbin, D. R. *J. Am. Chem. Soc.* **1992**, *114*, 3882.

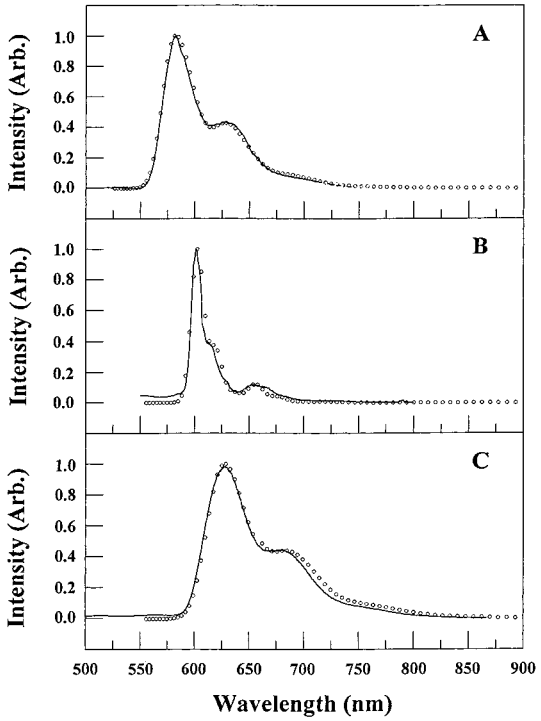

Figure 6. 77 K emission spectra of A [(bpy)$_2$Ru(**phen-nap**)]$^{2+}$, (B) [(bpy)$_2$Ru(**phen-pyr**)]$^{2+}$, and (C) [(bpy)$_2$Ru(**bpy-pyr**)]$^{2+}$ in 4:1 ethanol/methanol glasses. Solid lines represent fits to the data using eq 3 of text.

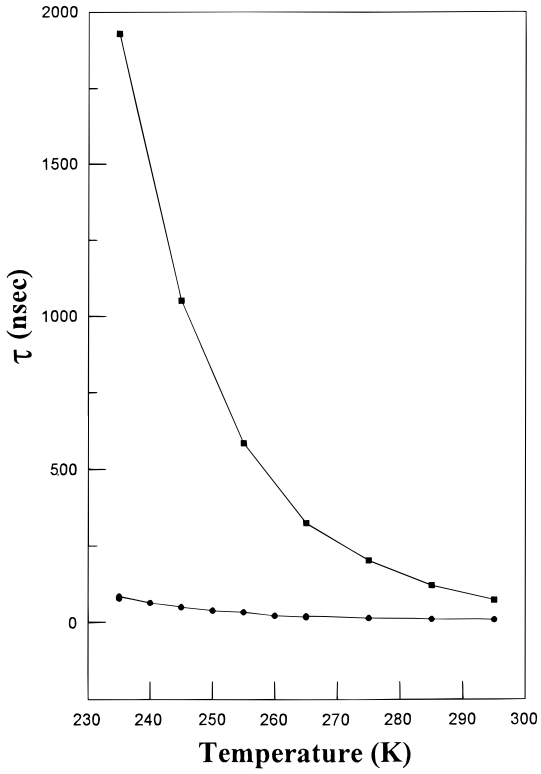

Figure 7. Temperature dependence of luminescence decays of [(bpy)$_2$Ru(**phen-pyr**)]$^{2+}$ (■) and [(bpy)$_2$Ru(**phen-nap**)]$^{2+}$ in CH_3CN between 235 K and room temperature. Decays fit a single exponential for both complexes in this temperature range.

the decay between 230 K and room temperature in CH_3CN is shown in Figure 7.

At all temperatures examined the luminescence spectra of [(bpy)$_2$Ru(**bpy-pyr**)]$^{2+}$ exhibit broad bands characteristic of emission from ^{3}MLCT states. The emission maxima in 4:1 ethanol/methanol at 77 K and at room temperature are lower in

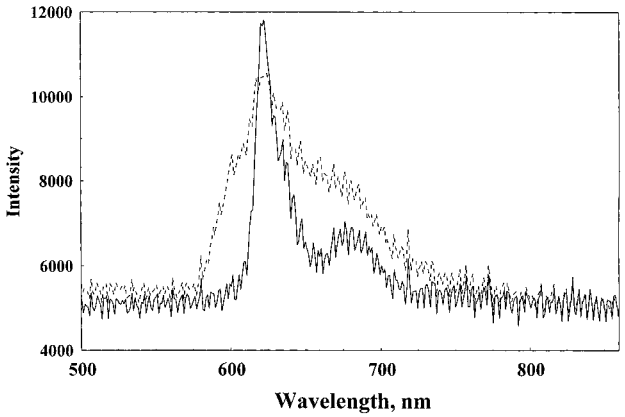

Figure 8. Gated emission spectra of $[(bpy)_2Ru(\textbf{phen-pyr})]^{2+}$ in 4:1 ethanol/methanol at 77 K following 460 nm excitation. Delay times are 0 (- - -, 10 μs gate) and 5 μs (—, 100 μs gate).

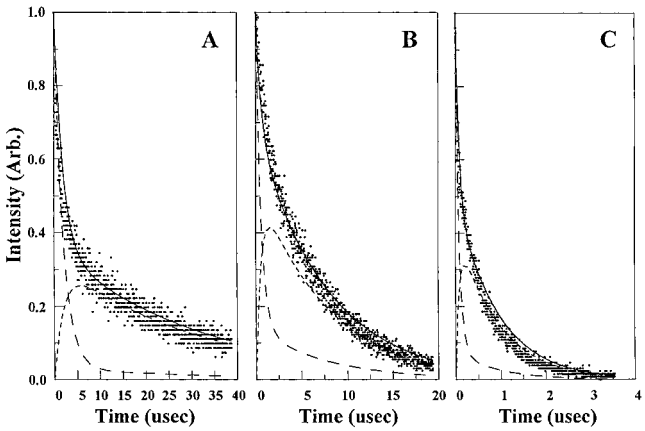

Figure 9. Luminescence decays of $[(bpy)^2Ru(\textbf{phen-pyr})]^{2+}$ in 4:1 ethanol/methanol at (A) 150, (B) 200, and (C) 250 K. The lines represent decays of the ^{3}MLCT state (long dash), the $^3(\pi \rightarrow \pi^*)$ state (short dash), and the overall decay (solid line) calculated using decay paths outlined in eq 4.

energy than the maxima of the ^{3}MLCT state of $[Ru(bpy)_3]^{2+}$ and the $^3(\pi\pi^*)$ state of **bpy-pyr**, suggesting the emission is from a ^{3}MLCT state localized on the **bpy-pyr** ligand. Luminescence decays at all temperatures can be fit as double exponentials, and representative decays at three temperatures are shown in Figure 10.

Discussion

Excited States of the Complexes. The simplest of the three complexes is $[(bpy)_2Ru(\textbf{phen-nap})]^{2+}$ since there is no ligand-localized excited state close in energy to the ^{3}MLCT state and excited state decays are single exponential at all temperatures examined. The naphthalene $^3(\pi \rightarrow \pi^*)$ state has an energy of approximately 21 000 cm^{-1},[26] well above the energy of the ^{3}MLCT state (Table 3). This complex serves as a model for the **phen-pyr** complex which is structurally very similar but has a pyrene $^3(\pi \rightarrow \pi^*)$ state nearly isoenergetic with the ^{3}MLCT state. The luminescence spectrum at room temperature and at 77 K has a bandshape characteristic of ^{3}MLCT emission in Ru(II) diimine complexes, and the calculated radiative decay rate constant is also consistent with ^{3}MLCT luminescence ($\eta_{isc}k_r$ of Table 2). In addition, the excited-state absorption spectrum shows bleaching of the Ru(II)(dπ) $\rightarrow$ bpy(π^*) MLCT transition in the 400−500 nm range (Figure 3C).

A key feature in the behavior of this complex is the large change in the luminescence lifetime between room temperature

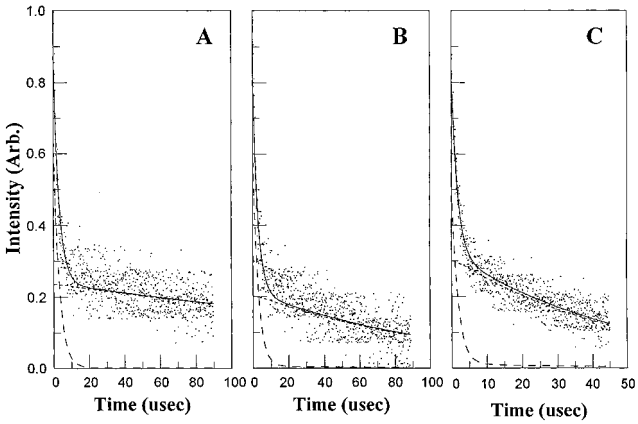

Figure 10. Luminescence decays of $[(bpy)_2Ru(\textbf{bpy-pyr})]^{2+}$ in 4:1 ethanol/methanol at (A) 150, (B) 200, and (C) 250 K. The lines represent decays of the ^{3}MLCT state (long dash), the $^3(\pi \rightarrow \pi^*)$ state (short dash), and the overall decay (solid line) calculated using decay paths outlined in eq 4.

and 230 K. Relative to the parent complex, $[(bpy)_2Ru(phen)]^{2+}$, this complex has a very short lifetime and low emission quantum yield at room temperature, indicating the existence of a unique nonradiative decay path. This type of behavior has been observed in other complexes having diimine ligands with substituents in the 6 position and results from a weakening of the ligand field induced by steric effects.[28] The weakened ligand field leads to a decrease in the energy of the ^{3}MC state, making thermally activated ^{3}MLCT $\rightarrow$ ^{3}MC internal conversion more facile (Scheme 1). The temperature dependence of the luminescence decay in the 230−300 K temperature range can be fit to a model which includes temperature-independent radiative and nonradiative components and a thermally activated decay process (eq 2). Fits of the data for $[(bpy)_2Ru(\textbf{phen-nap})]^{2+}$

$$1/\tau_{obs} = k_{obs}(T) = k_{r+nr} + k_0 \exp(-E_a/RT) \qquad (2)$$

(Figure 7) yield an activation energy of 1960 cm^{-1} and a prefactor, k_0, of (2 ± 1) × 10^{12} s^{-1}. Parameters of this magnitude are representative of ^{3}MLCT $\rightarrow$ ^{3}MC crossover in Ru(II) diimine complexes.[30] Upon cooling of the sample to 77 K, the luminescence lifetime and emission maximum are nearly the same as $[(bpy)_2Ru(phen)]^{2+}$ since the ^{3}MC state is no longer accessible via activated internal conversion.

The photophysical behavior of the **phen-pyr** complex is more difficult to interpret. The emission spectrum in room-temperature acetonitrile is structureless, and the calculated radiative decay rate constant is typical of ^{3}MLCT emission. However, the transient absorption spectrum of the complex has features which are not representative of Ru(II) diimine ^{3}MLCT states (Figure 3) and the lifetime of the transient absorbance is approximately 17 times longer than the luminescence lifetime. The transient absorption is positive at all wavelengths in the 400−650 nm range and has maxima at 430 and approximately 550 nm. The spectrum is very similar to the transient spectrum obtained by Ford and Rodgers for a donor−acceptor complex having a Ru(II) bipyridyl complex linked to pyrene by a hydrocarbon tether; the transient absorbance in this complex was assigned to a pyrene-localized $^3(\pi \rightarrow \pi^*)$ state.[10]

A separate issue involves assignment of localization of the ^{3}MLCT emission in this complex. From the spectroscopic and redox data available it is not clear whether the emission is of

(28) (a) Kelly, J. M.; Long, C.; O'Connell, C. M.; Vos, J. G.; Tinnemans, A. H. A. *Inorg Chem.* **1983**, *22*, 2818−25. (b) Rillema, D. P.; Macatangay, A.; Zheng, G. Y. *Inorg. Chem.* **1996**, *35*, 6823−6.

(29) Cooley, L. F.; Headford, C. E. L.; Elliott, C. M.; Kelley, D. F. *J. Am. Chem. Soc.* **1988**, *110*, 6673−82.

(30) Chang, Y.; Xu, X.; Yabe, T.; Yu, S.-C.; Anderson, D.; Orman, L.; Hopkins, J. *J. Phys. Chem.* **1990**, *94*, 729−36.

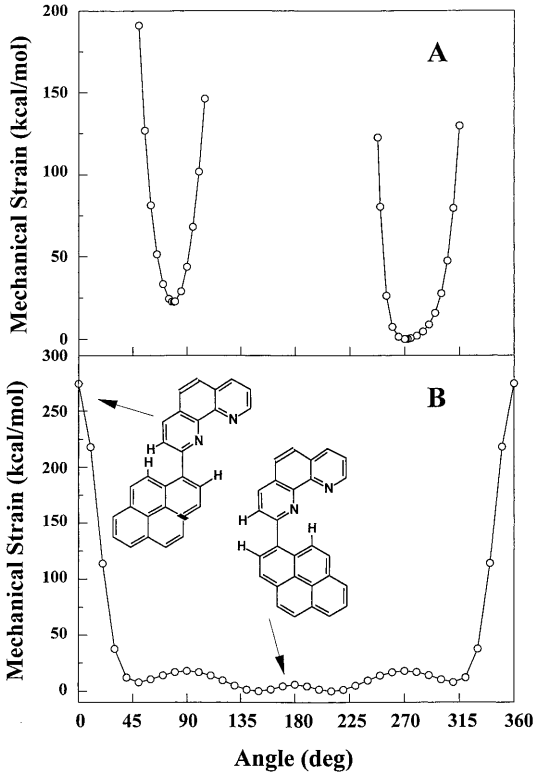

Figure 11. Strain energy as a function of the torsion angle between the phenanthroline and pyrene moieties for (A) $[(bpy)_2Ru(\textbf{phen-pyr})]^{2+}$ and (B) **phen-pyr**.

Ru(dπ) → bpy(π*) or Ru(dπ) → **phen-pyr**(π*) origin. Evidence in the literature suggests that the states can exist in equilibrium when the energy gap is small (< 500 cm^{-1}).[29] Time-resolved resonance Raman studies of related complexes do not help clarify assignment of excited-state localization for this complex. The parent complex $[(bpy)_2Ru(phen)]^{2+}$ has been shown to have a Ru(dπ) → bpy(π*) localized excited state[30] while the closely related complex $[(bpy)_2Ru(DIP)]^{2+}$ (DIP = 4,7-diphenylphenanthroline) has a ^{3}MLCT state localized on the DIP π* ligand.[31]

Quantitative interpretation of the spectroscopic data is complicated by the fact that $[(bpy)_2Ru(\textbf{phen-pyr})]^{2+}$ exists as a mixture of two atropisomers. Figure 11 shows the calculated strain energy of coordinated **phen-pyr** and the free ligand as a function of the torsion angle of the bond linking the pyrene and phenanthroline rings, clearly indicating the existence of two distinct atropisomers when the ligand is coordinated in a six-coordinate tris(diimine) complex.[32] The atropisomers are observed experimentally in ^{1}H NMR spectra of the complex.[33] Representations of the equilibrium conformations, in which the pyrene moiety is nearly perpendicular to the plane of the phenanthroline, are shown in Figure 12. It is clear that overlap of the pyrene and phenanthroline rings differs considerably for the two atropisomers, and it is conceivable that the two component photophysical behavior observed is the result of differing photophysics for the two atropisomers. Without separating the isomers, it is not possible to determine with certainty whether there is a difference between the two isomers.

(31) Kumar, C.; Barton, J.; Gould, I.; Turro, N.; Van Houten, J. *Inorg. Chem.* **1988**, *27*, 648−51.

(32) Strain energies were calculated by initially minimizing the energy of the molecule using the MM+ molecular mechanics routine associated with the program Hyperchem. Single point energies were then calculated for particular set torsion angles between the pyrene and the phenanthroline rings.

(33) Thummel, R. P. Unpublished results.

(34) Wacholtz, W. F.; Auerbach, R. A.; Schmehl, R. H. *Inorg. Chem.* **1986**, *25*, 227.

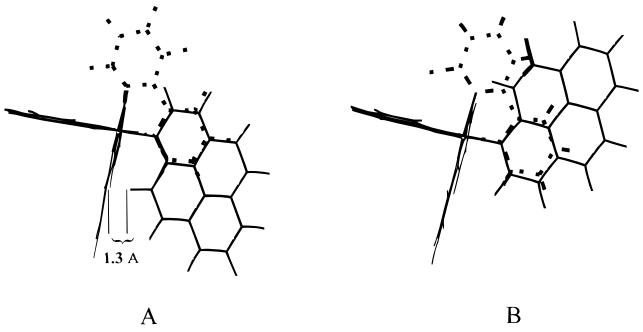

Figure 12. Representations of the atropisomers of $[(bpy)_2Ru(\textbf{phen-pyr})]^{2+}$ with torsion angles between the phenanthroline and pyrene of (A) 87 and (B) 273°. The framework of the bpy ligand π stacked with the pyrene moiety is shown with a dashed line.

However, the low-temperature luminescence behavior is independent of excitation wavelength, suggesting no significant difference exists in the absorption and following luminescence of the two isomers. In addition, the **phen-nap** complex also has two atropisomers and single exponential behavior is observed at all wavelengths and temperatures for the observed MLCT luminescence. Given these observations, the observed photophysical behavior of the **phen-pyr** complex was assumed to be due to factors other than the existence ot the two atropisomers.

If the observed photophysical behavior is the same for the two atropisomers, then both the ^{3}MLCT and $^3(\pi \rightarrow \pi^*)$ states have measureable lifetimes at room temperature but are not in equilibrium. The excited-state decay of the **phen-pyr** complex following excitation into the MLCT state can be described as shown in Scheme 1; the dynamics of the reversible energy transfer are discussed later.

The steady-state luminescence of of $[(bpy)_2Ru(\textbf{phen-pyr})]^{2+}$ at 77 K clearly arises from a pyrene $^3(\pi \rightarrow \pi^*)$ state. The spectrum has a very narrow 0−0 band and bears a strong resemblence to pyrene phosphorescence in frozen matrices.[27] The luminescence decay, however, is double exponential (Table 2), and time-resolved emission spectra clearly show that the spectrum of the short component is broader, more closely resembling emission from the ^{3}MLCT state of the complex. The long-lived component of the emission has a lifetime in excess of 5 ms; the lifetime of pyrene triplet in polar matrices is 11 ms.[26] A significant point is that the steady-state emission spectrum of $[(bpy)_2Ru(\textbf{phen-pyr})]^{2+}$ at 77 K differs markedly from that of **phen-pyr** (Figures 5 and 6). This is surprising since intraligand phosphorescence has been observed from numerous Re(I), Pt(II), and Rh(III) complexes and, in virtually every case, very little difference is observed between the spectrum of the coordinated ligand and the free ligand.[7−9] In the case of **phen-pyr**, the luminescence of the complex more closely resembles that of unsubstituted pyrene than the phosphorescence of the free ligand. The major difference between the free ligand and the complexed ligand is that the torsion angle between the phenanthroline and pyrene moieties is rigidly fixed in the complex (Figure 11). The implication from the spectral data is that the pyrene does not exhibit any significant electronic interaction with the phenanthroline when constrained to be nearly orthogonal to the coordinated phenanthroline.

The temperature dependence of the luminescence of $[(bpy)_2Ru(\textbf{phen-pyr})]^{2+}$ exhibits two distinct regions. Between 220 and 300 K, the luminescence decay can be fit as a single exponential and is strongly temperature dependent while at lower temperatures the decay can only be fit as a double exponential and each decay component changes more gradually with temperature. In the higher temperature region, the principal nonradiative decay path of the ^{3}MLCT state is very likely internal conversion

to the ^{3}MC state. Relaxation of the ^{3}MLCT state via population of the ^{3} MC state should be at least as facile as the same process in $[(bpy)_2Ru(\textbf{phen-nap})]^{2+}$ (Scheme 1). If it is assumed that the temperature dependence of the luminescence lifetime above 220 K can be attributed exclusively to thermally activated population of a ^{3}MC state, lifetimes can be fit to eq 2 to yield an activation energy of 2600 cm^{-1} and a prefactor, k_0, of 5×10^{12} s^{-1} (Figure 7); these parameters are representative of values obtained for ^{3} MLCT $\rightarrow$ ^{3}MC state internal conversion observed in other Ru(II) diimine complexes.[20,35]

In an attempt to obtain independent evidence for population of the ^{3}MC state, the complexes were photolyzed in CH_2Cl_2 solutions containing Cl^- ion. It is known that $[Ru(bpy_3)]^{2+}$ readily photolyzes to yield $[Ru(bpy)_2Cl_2]$ in CH_2Cl_2 while mixed-ligand complexes having inaccessible ^{3}MC states are photoinert under the same conditions.[34] Both the **phen-nap** and **phen-pyr** complexes readily undergo photolysis to yield cis-chloro complexes. Examination of the photolysis products of $[(bpy)_2Ru(\textbf{phen-pyr})](PF_6)_2$ by luminescence spectroscopy clearly indicates the loss of the **phen-pyr** ligand since fluorescence from the noncoordinated **phen-pyr** ligand is observed.

The **bpy-pyr** complex is spectroscopically very different from the **phen-pyr** complex. It is strongly luminescent at room temperature, and the broad, structureless emission has a maximum which is lower in energy than that of either $[Ru(bpy)_3]^{2+}$ or $[(bpy)_2Ru(\textbf{phen-pyr})]^{2+}$, consistent with luminescence originating from a Ru(dπ) $\rightarrow$ **bpy-pyr** (π^*) ^{3}MLCT state. In addition, the molar absorptivity of the MLCT transition of the complex is relatively large and may reflect extension of the transition dipole onto the pyrene substituent. Unlike the **phen-pyr** ligand, the coordinated **bpy-pyr** has energetically accessible conformations that make delocalization of the MLCT state onto the pyrene ligand possible. The luminescence decay is double exponential at room temperature with a long component of over 50 μs in acetonitrile; time-resolved emission spectra reveal no change in the spectrum during the lifetime of the decay. The radiative decay rate constant calculated from the quantum yield and the short component of the luminescence decay is 7.5×10^4 s^{-1} and is typical for ^{3}MLCT states.[20,35] If the radiative decay rate constant is determined using the long decay component and the observed emission quantum yield, the value is 1700 s^{-1}. The excited-state absorption spectrum also differs from that of both the **phen-pyr** complex and $[Ru(bpy)_3]^{2+}$. The spectrum evolves in time, losing the bleach in the 350−400 nm region observed at times less than 1 μs while maintaining the absorption in the red (see Figure 3b). One explanation for this behavior is that excitation leads to a mixture of ^{3}MLCT and $^3(\pi \rightarrow \pi^*)$ states which is rich in the ^{3}MLCT state (bleaching in thd 360−400 nm region) and evolves to a mixture in which the predominant species is the pyrene $^3(\pi \rightarrow \pi^*)$ state.

At 77 K, the emission spectrum of $[(bpy)_2Ru(\textbf{bpy-pyr})]^{2+}$ (Figure 6) is characteristic of ^{3}MLCT state emission of Ru(II) diimine complexes. The luminescence decay can be fit to a double exponential having components of 4.1 and 650 μs; the spectral band shape does not change over the measureable decay of the excited state.

Energy Gaps between $^3(\pi \rightarrow \pi^*)$ and ^{3}MLCT States. Determination of the relative energy levels of both long-lived excited states of the two pyrene-containing complexes can be clarified by analysis of the Franck−Condon factors associated with excited state relaxation in the complexes and free ligands. These can be extracted from 77 K luminescence spectra, which exhibit a clearly defined vibrational progression for each complex. The spectra were fit using a Franck−Condon analysis employing eq 3. The procedure for fitting data has been

$$I(\bar{\nu}) = \sum_M \sum_L \left(\frac{E_0 - Mh\nu_m - Lh\nu_l}{E_0}\right)^3 \left(\frac{S_m^M}{M!}\right)\left(\frac{S_l^L}{L!}\right) \times \left\{\exp\left[-4(\ln 2)\left(\frac{\bar{\nu} - E_0 + Mh\nu_m + Lh\nu_l}{\Delta\bar{\nu}_{1/2}}\right)^2\right]\right\} \quad (3)$$

described in detail by Meyer and co-workers.[36] The model includes the 0−0 emission energy, E_0, averaged low- and medium-frequency acceptor modes, $h\nu_l$ and $h\nu_m$, the electron−vibrational coupling constant, S, for both the low- and medium-frequency modes, and the full-width half-maximum of the individual vibronic components, $\nu_{1/2}$.

In the fitting of the data for Figure 6, values of $h\nu_l$ and S_l were fixed and spectra were optimized for the parameters E_0, S_m, $h\nu_m$, and $\Delta\nu_{1/2}$; the calculated spectra are shown in Figure 6, and the parameters are given in Table 3. Values listed for the free ligands **phen-pyr** and **bpy-pyr** are estimated from the spectra of Figure 5; the values of E_0 are obtained from the maximum of the highest energy vibronic component and thus represent a lower limit value for E_0, and the values of $h\nu_m$ are obtained from the spacing between maxima of the vibronic components.

From the results an estimate of the relative energy of the ^{3}MLCT and $^3(\pi \rightarrow \pi^*)$ states of the complexes in frozen matrices can be obtained. For the **phen-pyr** complex, the emission is from the $^3(\pi \rightarrow \pi^*)$ state; E_0 is found to be 16 500 cm^{-1}. The emission maximum of the free **phen-pyr** ligand phosphorescence is 16 100 cm^{-1} and the band shape clearly differs from the phosphorescence of the coordinated ligand. An estimate of the ^{3}MLCT emission energy of the **phen-pyr** complex at 77 K can be obtained by assuming the MLCT state energies of the **phen-pyr** and the **phen-nap** complexes are the same. With this approximation, Table 3 indicates that the ^{3}MLCT state is approximately 700 cm^{-1} higher in energy than the $^3(\pi \rightarrow \pi^*)$ state of the coordinated **phen-pyr** in low-temperature glasses.

The relative energies of the triplet states in the **bpy-pyr** complex can be estimated from the phosphorescence spectrum of the ligand and the luminescence of the complex. Assuming the $^3(\pi \rightarrow \pi^*)$ state energy of the ligand does not change upon coordination, the ^{3}MLCT state is approximately 200 cm^{-1} lower in energy than the **bpy-pyr** $^3(\pi \rightarrow \pi^*)$ state. The relative state energies for the three complexes are shown in Figure 13.

If it is assumed that entropy changes associated with forming the excited states are small, the energy gaps determined above can be used as free energies to determine equilibrium constants (K_{en}) at 77 K for ^{3}MLCT to $^3(\pi \rightarrow \pi^*)$ energy transfer. Values of K_{en} obtained are 5×10^5 for the **phen-pyr** complex and 0.024 for the **bpy-pyr** complex. If the energy gap remains unchanged between 77 K and room temperature, the equilibrium constants are 29 for the **phen-pyr** complex and 0.40 for the **bpy-pyr** complex. It is known, however, that E_0 values for ^{3}MLCT states of Ru(II) diimine complexes are higher in frozen matrices than in solutions; this would have the effect of making both equilibrium constants smaller.

The photophysical behavior of $[(bpy)_2Ru(\textbf{phen-nap})]^{2+}$, $[(bpy)_2Ru(\textbf{phen-pyr})]^{2+}$, and $[(bpy)_2Ru(\textbf{bpy-pyr})]^{2+}$ at a given temperature can be summarized by considering the relative energies and internal conversion dynamics of the ^{3}MLCT state, the ^{3}pyr ($^3(\pi \rightarrow \pi^*)$) state, and the triplet metal-centered (^{3}MC) state. Qualitative state diagrams for each of the three

(35) Meyer, T. J. *Pure Appl. Chem.* **1986**, *58*, 1193−206.
(36) (a) Kober, E. M.; Caspar, J. V.; Lumpkin, R. S.; Meyer, T. J. *J. Phys. Chem.* **1986**, *90*, 3722. (b) Murtaza, Z.; Graff, D. K.; Zipp, A. P.; Worl, L. A.; Jones, W. E., Jr.; Bates, W. D.; Meyer, T. J. *J. Phys. Chem.* **1994**, *98*, 10504.

Table 4. Parameters Obtained in Fits of Luminescence Decays in 4:1 Ethanol/Methanol Solutions Using Reversible Energy Transfer Model

$[(bpy)_2Ru(L)]^{2+}$ complex	temp, K	η^0 CT	k_{CT}, × 10^5 s^{-1}	k^0_{dd}, × 10^{13} s^{-1}	$E_{a,dd}$, cm^{-1}	$k_{dd}(T)$, × 10^5 s^{-1}	η^0 π	k^0_{π}, × 10^3 s^{-1}	$E_{a,\pi}$, cm^{-1}	k^0_{en}, × 10^6 s^{-1}	$E_{a,en}$, cm^{-1}	ΔE_{en}, cm^{-1}	$k_{en}(T)$, × 10^5 s^{-1}
phen-pyr	150	1	2.4	1.9	2590	0.03	0	2.2	300	4.8	350	−125	1.7
	200	1	3.2	2.2	2570	2.0	0	2.2	330	4.5	200	−135	10.6
	250	1	3.1	2.1	2640	53.0	0	2.2	360	6.0	65	−165	41.3
bpy-pyr	150	0.73	6.4				.27	2.9	270	1.1	635	97	0.02
	200	0.76	6.9				.24	3.0	310	0.96	650	98	0.1
	250	0.62	14.0				.38	3.0	305	0.88	590	100	0.3

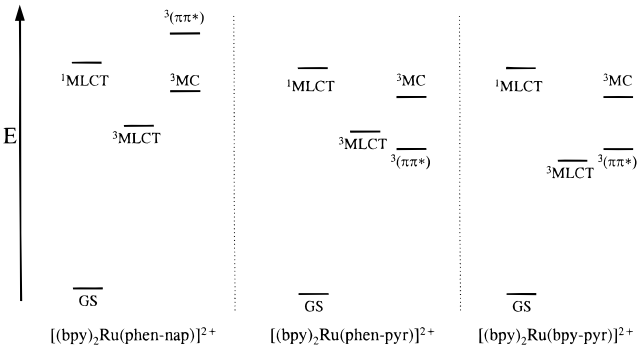

Figure 13. Relative energy level diagrams for (A) $[(bpy)_2Ru)$(**phen-nap**)$]^{2+}$, (B) $[(bpy)_2Ru$(**phen-pyr**)$]^{2+}$, and (C) $[(bpy)_2Ru$(**bpy-pyr**)$]^{2+}$.

complexes can be generated from the available spectroscopic data (Figure 13). The important differences are that (a) the $^3(\pi \rightarrow \pi^*)$ state of the **phen-nap** complex is much higher in energy than the other two states and is not involved in the excited state relaxation dynamics, (b) all three triplet states influence the decay kinetics of the **phen-pyr** complex, and (c) the ^{3}MC state of the **bpy-pyr** complex is much higher than the other two triplet states and does not exist as a relaxation path at temperatures between 77 K and room temperature.

Reversible Energy Transfer. From the double exponential luminescence decays of the **phen-pyr** complex at temperatures between 77 and 200 K and the **bpy-pyr** complex at all temperature measured, it is clear that multiple excited states exist concomitantly (Figures 8−10). Given the small energy gaps between the ^{3}MLCT and $^3(\pi \rightarrow \pi^*)$ states of the two complexes, it is possible that the double exponential decays result either from luminescence from both states or luminescence from a single state in which the fast exponential component reflects pre-equilibrium relaxation of the emitting state and the longer decay process involves relaxation of the equilibrated states. At 77 K the behavior of the **phen-pyr** complex is clear since the time-resolved emission spectrum shows the presence of luminescence from the ^{3}MLCT state at times less than 10 μs and the narrow, structured $^3(\pi \rightarrow \pi^*)$ luminescence exclusively at longer times (Figure 8). At temperatures above the glass transition temperature of the matrix (>130 K) the decays remain double exponential but the structured $^3(\pi \rightarrow \pi^*)$ luminescence at long times is no longer observed. The **bpy-pyr** complex has both steady-state and time-resolved spectra representative of luminescence from a ^{3}MLCT state at all temperatures between 77 K and room temperature. Thus, between 130 and 200 K, the luminescence decays of both complexes can be fit by assuming emission is exclusively from the ^{3}MLCT state and the double exponentiality results from a rapid decay of the initially formed ^{3}MLCT state and a slower decay associated with ^{3}MLCT emission following internal conversion from the $^3(\pi \rightarrow \pi^*)$ state.

In considering energy transfer in the two pyrene-containing complexes at temperatures near room temperature, the equilibrium constants are within a factor of 30 of unity. For the **phen-pyr** complex, the ratio of rate constants for decay of the ^{3}MLCT and $^3(\pi \rightarrow \pi^*)$ states, obtained independently from luminescence and transient absorbance decays, is 17 (Table 2), which is close to the estimated room-temperature equilibrium constant (*vide supra*). Thus, it is possible that excited-state decay in this complex involves competitive relaxation to the ground state and forward energy transfer for the ^{3}MLCT state and relaxation of the $^3(\pi \rightarrow \pi^*)$ state via energy transfer to the MLCT state. The rate constant for energy transfer from the ^{3}MLCT state to the $^3(\pi \rightarrow \pi^*)$ state can be estimated to be approximately 10^8 s^{-1} $(29(1/\tau_{TA}(298)))$, one-fourth the observed nonradiative relaxation rate constant of the ^{3}MLCT state. In the **bpy-pyr** complex the $^3(\pi \rightarrow \pi^*)$ state is higher in energy than the ^{3}MLCT state ($K_{en} < 1$); as a result the rate constant for energy transfer from the ^{3}MLCT state to the $^3(\pi \rightarrow \pi^*)$ state must be less than the measured rate constant for decay of the $^3(\pi \rightarrow \pi^*)$ state, 2×10^4 s^{-1}. The vast difference in energy transfer rate constants of the two complexes cannot be rationalized solely in terms of differences in the energy gaps for the two processes.

To explore this difference in greater detail, the luminescence behavior of both complexes was investigated at several temperatures and the decays were analyzed in terms of the processes outlined in Scheme 1. The scheme shows rate constants used to analyze the decay and interconversion of the ^{3}MLCT and $^3(\pi \rightarrow \pi^*)$ states. The relaxation of the ^{3}MC state is assumed to be rapid relative to back internal conversion to populate the ^{3}MLCT state; this assumption has been used extensively in analysis of the temperature dependence of luminescence decays of ^{3}MLCT states.[20a] The rate constants for decay of the two long lived excited states can be written as shown in eq 4. The

$$k_{CT} = \left[k_{CT0} + k_{dd}\exp\left(-\frac{E_{a,dd}}{RT}\right) + k_{en0}\exp\left(-\frac{E_{a,en}}{RT}\right)\right] - \left[k_{en0}\exp\left(-\frac{E_{a,en}-\Delta E}{RT}\right)\right]$$

$$k_{\pi} = \left[k_{pi0}\exp\left(-\frac{E_{a,\pi}}{RT}\right) + k_{en0}\exp\left(-\frac{E_{a,en}-\Delta E}{RT}\right)\right] - \left[k_{en0}\exp\left(-\frac{E_{a,en}}{RT}\right)\right] \quad (4)$$

luminescence decays at each temperature shown in Figures 9 and 10 were fit to a coupled excited-state model which includes intersystem crossing from the initially formed ^{1}MLCT state to both the ^{3}MLCT and $^3(\pi \rightarrow \pi^*)$ states, η^0_{CT} and η^0_{π}, respectively.

Whether or not the two states exist in equilibrium depends on the relative magnitude of the rate constants for decay of the excited states to the ground state and the forward and reverse energy transfer rate constants. Decays of the **phen-pyr** complex were fit by assuming intersystem crossing to the ^{3}MLCT state occurs with unit efficiency ($\eta^0_{CT} = 1$). The fit of the decay included (1) thermally activated ^{3}MLCT to ^{3}MC internal conversion, (2) thermally activated nonradiative decay of the $^3(\pi \rightarrow \pi^*)$ state, and (3) energy transfer with k_{en0}, $E_{a,en}$, and ΔE_{en} as parameters. Values for ^{3}MLCT to ^{3}MC internal conversion rates were approximated by using values for the same process observed for the **phen-nap** complex.

Analysis of decays for the **bpy-pyr** complex required intersystem crossing from the ^{1}MLCT state to both the ^{3}MLCT and $^3(\pi \rightarrow \pi^*)$ states but omitted the ^{3}MLCT to ^{3}MC internal conversion. Direct intersystem crossing from the ^{1}MLCT state to the pyrene $^3(\pi \rightarrow \pi^*)$ state must be included for this complex because a very long lived component to the luminescence exists despite the fact that the endergonic energy transfer from the ^{3}MLCT state to the pyrene $^3(\pi \rightarrow \pi^*)$ state is slow relative to nonradiative relaxation of the ^{3}MLCT state at temperatures below 250 K.

Table 4 summarizes parameters obtained from the fits at three different temperatures, and the calculated decays are shown along with the experimental results in Figures 9 and 10. The prefactor for the **phen-pyr** complex is larger than that of the **bpy-pyr** complex by approximately a factor of 5. Thus, while both prefactors are quite small and indicate relatively weak electronic coupling between the two states, the **phen-pyr** complex appears to be somewhat more strongly coupled. In addition, the activation energy extracted from the fits of the decays is significantly larger for the **bpy-pyr** complex, even considering the free energy difference. The fits suggest that both electronic and nuclear factors contribute to more efficient energy transfer in the **phen-pyr** complex. Finally, the results are consistent with the behavior in frozen matrices. The rate constant for uphill energy transfer in the **bpy-pyr** complex cannot compete with radiative and nonradiative decay of the ^{3}MLCT state, and the $^3(\pi \rightarrow \pi^*)$ state decays via energy transfer to the MLCT triplet. In the **phen-pyr** complex the ^{3}MLCT state decays via both luminescence and energy transfer pathways yielding a very long lived pyrene-localized $^3(\pi \rightarrow \pi^*)$ state which is luminescent.

Conclusions

For both the pyrenyl complexes studied, the ^{3}MLCT excited state of the Ru(II) diimine complex and the $^3(\pi \rightarrow \pi^*)$ state of the pyrenyl substituent are nearly isoenergetic; the ^{3}MLCT state is the lowest energy state for the **bpy-pyr** complex, and the pyrene $^3(\pi \rightarrow \pi^*)$ state is lower in energy for the **phen-pyr** complex. Kinetic analysis of luminescence decays clearly shows that the exchange energy transfer is slower than relaxation of the ^{3}MLCT state in both complexes but more rapid than decay of the $^3(\pi \rightarrow \pi^*)$ state. This is true regardless of the model used to fit the double exponential decays obtained over a wide temperature range. Decay of the ^{3}MLCT state of the **bpy-pyr** complex is so much faster than energy transfer that the only route to forming the $^3(\pi \rightarrow \pi^*)$ state is via direct intersystem crossing from the selectively excited ^{1}MLCT state.

Acknowledgment. R.H.S. wishes to acknowledge support from the Department of Energy, Office of Basic Energy Sciences (Grant DE-FG02-96ER14617), and the Tulane Center for Photoinduced Processes, funded by the National Science Foundation and the Louisiana Board of Regents. R.P.T. wishes to acknowledge the support of the Robert A. Welch Foundation and the National Science Foundation (Grant CHE-9224686). P.P. acknowledges support from the Department of Energy, Office of Basic Energy Sciences (DE-FG05-92ER14310).

JA970069F